

# Impurity photovoltaic effect in GaAs solar cell with two deep impurity levels

Samira Khelifi<sup>a,b,\*</sup>, Marc Burgelman<sup>a,2</sup>, Johan Verschraegen<sup>a,2</sup>, Abderrahmane Belghachi<sup>b,1</sup>

<sup>a</sup> Department of Electronics and Information Systems (ELIS), University of Gent, Pietersnieuwstraat 41, B-9000 Gent, Belgium

<sup>b</sup> Laboratory of Semiconductor Devices Physics (LPDS), Physics Department, University of Béchar, POB 417, Béchar, Algeria

## ARTICLE INFO

### Article history:

Received 12 December 2007

Received in revised form

30 June 2008

Accepted 1 July 2008

Available online 6 August 2008

### Keywords:

GaAs solar cell

IPV effect

SCAPS-1D

Light trapping

## ABSTRACT

The impurity photovoltaic (IPV) effect has been extensively investigated for silicon solar cells with indium impurities. A small positive effect on the efficiency was theoretically predicted, provided that efficient light trapping schemes are applied. Since IPV effects are predicted to be more pronounced in wider band gap materials and possibly also by introducing more than one impurity level, we carried out a numerical study on GaAs solar cells with copper impurities. Indeed, copper introduces multiple acceptor type mid-gap levels in GaAs, two of which are investigated here: one at 0.14 eV and another at 0.40 eV above the valence band edge. We used a solar cell device simulator (SCAPS) specially adapted to include the IPV effect. We varied the impurity concentration and the light trapping parameters of the device, and calculated the occupation probability of the impurity levels, the generation and recombination through these levels (thermal and optical) and the solar cell characteristics: quantum efficiency,  $QE(\lambda)$ , short-circuit current  $J_{sc}$ , open-circuit voltage  $V_{oc}$  and efficiency  $\eta$ .

A significant IPV effect with extended response in the infrared is calculated when efficient light trapping is present. When an internal reflection coefficient  $R = 0.99$  can be reached at both the front and the back surface of the solar cell, an increase of the short-circuit current densities 2 mA/cm<sup>2</sup> can be obtained. The consequences of two levels instead of one are calculated and discussed, leading to a trade-off between  $J_{sc}$  improvement and a  $V_{oc}$  decrease.

© 2008 Elsevier B.V. All rights reserved.

## 1. Introduction

The principle of the impurity photovoltaic (IPV) effect is based on incorporating of impurities with energy levels somewhere in the band gap of the material. This can hence provide additional photons transitions from the valence band to the conduction band by absorption of two or more photons with energies less than the band gap.

The IPV effect in silicon solar cells with indium impurity defects has been theoretically and numerically treated in several literature reports [1–3]. It was shown that the incorporation of indium impurities into silicon, together with the use of light trapping, leads to an increase in short-circuit current, but at the same time to a degradation in the open-circuit voltage. However, theoretical calculations show that the IPV effect is more attractive for solar cells with larger band gap materials [4].

In previous work [5,6] we have presented new results obtained for the IPV effect in silicon solar cells using the software SCAPS [7], which was extended to include this effect. The main new features being implemented in this SCAPS version are: (i) the occupation probability of the defects depends on their optical capture cross section for electrons and holes; (ii) the optical absorption coefficient accounts for photoemission electrons and holes from the IPV impurity, and hence becomes position dependent; (iii) the optical capture cross sections are either taken from a file or calculated analytically according to a model by Lucovsky [8]; and (iv) a simple light trapping scheme have been implemented.

In this work we reinvestigate the potential of the IPV effect in wide band gap materials, such as gallium arsenide containing copper impurities. Copper impurities in GaAs introduce several more or less deep acceptor states with reported energy levels of 0.13–0.15, 0.24 and 0.40–0.49 eV above the valence band edge [9–15]; however, the exact structure of these levels are not known [15]. The possible IPV effect in copper doped GaAs solar cells is investigated here numerically with SCAPS: the current–voltage ( $J$ – $V$ ) characteristics and the internal quantum efficiency ( $QE(\lambda)$ ) are calculated and the influence of some determining parameters is discussed. We investigated the influence of the density of the Cu defects and the light trapping parameters of the solar cell structure. The contribution of the various Cu levels is assessed

\* Corresponding author at: Department of Electronics and Information Systems (ELIS), University of Gent, Pietersnieuwstraat 41, B-9000 Gent, Belgium. Tel.: +32 9 264 3381; fax: +32 9 264 3594.

E-mail addresses: [samira\\_khelifi@yahoo.fr](mailto:samira_khelifi@yahoo.fr), [Samira.Khelifi@elis.ugent.be](mailto:Samira.Khelifi@elis.ugent.be) (S. Khelifi).

<sup>1</sup> Tel.: +213 49810324; fax: +213 49815244.

<sup>2</sup> Tel.: +32 9 264 3381; fax: +32 9 264 3594.

by considering all combinations of two of the defects, and then studying the effect of the most efficient couple of defects in more detail.

## 2. Theory of IPV effect

In the simple Shockley–Read–Hall (SRH) recombination model, electrons and holes are captured and excited thermally from an impurity with an energy level inside the semiconductor band gap. To include the IPV effect, this model is extended with two impurity optical transitions as shown in Fig. 1. The modified SRH expression is then given by [1]

$$U = \frac{np - (n_1 + \tau_{n0}g_{nt})(p_1 + \tau_{p0}g_{pt})}{\tau_{n0}(p + p_1 + \tau_{p0}g_{pt}) + \tau_{p0}(n + n_1 + \tau_{n0}g_{nt})} \quad (1)$$

with

$$\tau_{n0} = \frac{1}{c_n N_t} \quad \text{and} \quad \tau_{p0} = \frac{1}{c_p N_t} \quad (2)$$

$$n_1 = N_C e^{-(E_C - E_t)/kT}, \quad p_1 = N_V e^{-(E_t - E_V)/kT} \quad (3)$$

$$g_{nt} = N_t \int_{\lambda_{n \min}}^{\lambda_{n \max}} \sigma_n^{\text{opt}}(x, \lambda) \phi_{ph}(x, \lambda) d\lambda \quad (4)$$

$$g_{pt} = N_t \int_{\lambda_{p \min}}^{\lambda_{p \max}} \sigma_p^{\text{opt}}(x, \lambda) \phi_{ph}(x, \lambda) d\lambda \quad (5)$$

$$\phi_{ph}(x, \lambda) = \phi_{\text{ext}}(\lambda) \frac{1 + R_b e^{-2\alpha_{\text{tot}}(\lambda)(L-x)}}{1 - R_f R_b e^{-2\alpha_{\text{tot}}(\lambda)L}} e^{-\alpha_{\text{tot}}(\lambda)x} \quad (6)$$

In Eq. (1),  $n$  and  $p$  are the electron and hole concentrations,  $\tau_{n0}$  and  $\tau_{p0}$  are the SRH lifetimes for electrons and holes,  $c_n$  and  $c_p$  are the electron and hole thermal capture cross sections,  $N_t$  is the impurity concentration, and  $E_t$  is the impurity level energy. The electron and hole concentrations  $n_1$  and  $p_1$  in Eq. (3) are calculated with the Fermi level coinciding with the impurity level,  $E_C$  and  $E_V$  are the conduction and valence band edges, and  $N_C$  and  $N_V$  are the effective densities of states in the conduction and valence bands. The optical emission rates from the impurity,  $g_{nt}$  for electrons and  $g_{pt}$  for holes constitute the IPV extension to the normal SRH expression. In Fig. 1, these processes are indicated as  $E_e^{\text{opt}}$  and  $H_e^{\text{opt}}$ , respectively. Eq. (1) takes into account that the

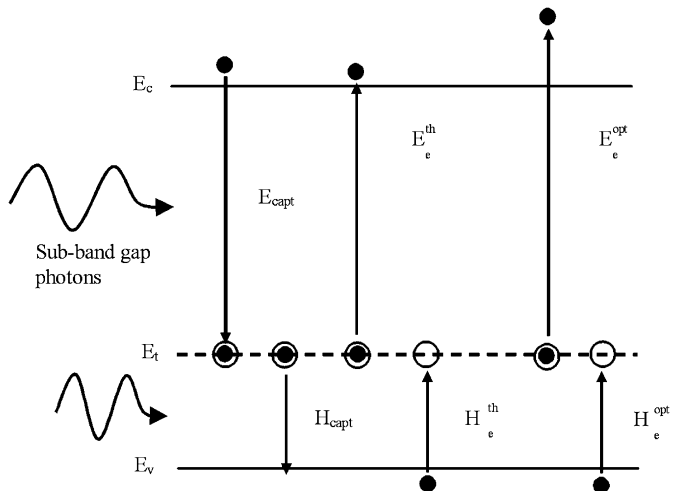


**Fig. 1.** Transitions between an IPV defect level and the conduction and valence bands: thermal capture ( $E_{\text{capt}}$  and  $H_{\text{capt}}$ ), thermal emission ( $E_e^{\text{th}}$  and  $H_e^{\text{th}}$ ) and the optical IPV emission ( $E_e^{\text{opt}}$  and  $H_e^{\text{opt}}$ ), where  $E$  stands for electrons and  $H$  for holes.

impurity should be fully occupied for the optical electron emission process ( $E_e^{\text{opt}}$ , with optical cross section  $\sigma_n^{\text{opt}}(\lambda)$ ) and completely empty for the optical hole emission process ( $H_e^{\text{opt}}$ , with optical cross section  $\sigma_p^{\text{opt}}(\lambda)$ ) [1].

Eqs. (4) and (5) are given for a normal incident light, without considering the increase of the optical path length by Lambertian or other scattering at the surfaces [1]. The external incident photon flux is  $\phi_{\text{ext}}(\lambda)$  and spectral distribution of the photon flux at distance  $x$  from the illuminated surface is noted as  $\phi_{ph}(x, \lambda)$ . In Eq. (6),  $L$  is the total length of the solar cell, and  $R_f$  and  $R_b$  are the internal reflection coefficients at the front and back of the cell, respectively. Setting  $R_f$  and  $R_b$  equal to zero corresponds to a solar cell without internal reflection, while a maximum (but unphysical) internal reflection is obtained by setting  $R_f$  and  $R_b$  equal to unity.

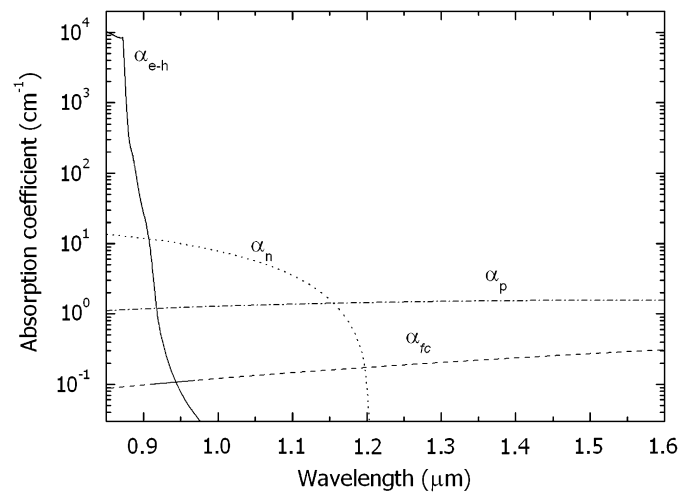


**Fig. 2.** Optical absorption coefficients as a function of wavelength calculated with the Cu(B) level and for  $N_D = N_t(B) = 10^{17} \text{ cm}^{-3}$  and  $R_f = 0.999$  and  $R_b = 0.9999$ .  $\alpha_{e-h}$  is the band-to-band absorption coefficient,  $\alpha_n$  defect to conduction band absorption coefficient,  $\alpha_p$  valence band to defect level absorption coefficient and  $\alpha_{fc}$  free carrier absorption coefficient.

**Table 1**

GaAs and copper parameters used in simulation at  $T = 300 \text{ K}$

Property	Symbol	Value	Unit	Ref.
GaAs band gap energy	$E_g$	1.42	eV	[17]
Dielectric constant	$\epsilon_r$	13.18		[10]
Electron mobility	$\mu_n$	4600	$\text{cm}^2/\text{V s}$	[10]
Hole mobility	$\mu_p$	239	$\text{cm}^2/\text{V s}$	[10]
Electron effective mass	$m_n^*/m_0$	0.063		[17]
Hole effective mass	$m_p^*/m_0$	0.45		[17]
Refractive index	$n$	3.3		[17]
Surface recombination velocity	$S_n = S_p$	$10^4$	cm/s	[18,19]
<b>Cu(A) defect level</b>				
Energy level above $E_V$	$E_t(A) - E_V$	0.14	eV	[10,20]
Electron capture cross section	$\sigma_n^{\text{th}}(A)$	$\leq 10^{-20}$	$\text{cm}^2$	[21,22]
Hole capture cross section	$\sigma_p^{\text{th}}(A)$	$1.20 \times 10^{-17}$	$\text{cm}^2$	[20]
<b>Cu(B) defect level</b>				
Energy level above $E_V$	$E_t(B) - E_V$	0.40	eV	[12–14,20,22]
Electron capture cross section	$\sigma_n^{\text{th}}(B)$	$\leq 10^{-20}$	$\text{cm}^2$	[21,22]
Hole capture cross section	$\sigma_p^{\text{th}}(B)$	$6.30 \times 10^{-15}$	$\text{cm}^2$	[12,14]
<b>Cu(C) defect level</b>				
Energy level above $E_V$	$E_t(C) - E_V$	0.24	eV	[9,10]
Electron capture cross section	$\sigma_n^{\text{th}}(C)$	$10^{-22}$	$\text{cm}^2$	
Hole capture cross section	$\sigma_p^{\text{th}}(C)$	$2.7 \times 10^{-16}$	$\text{cm}^2$	

In SCAPS the parameters  $R_b$  and  $R_f$  are used to describe empirically light trapping without getting into the details of how this light trapping is achieved.

The total absorption coefficient is the sum of all absorption processes in the cell

$$\alpha_{\text{tot}}(\lambda) = \alpha_{e-h}(\lambda) + \alpha_n(\lambda) + \alpha_p(\lambda) + \alpha_{fc}(\lambda) \quad (7)$$

where  $\alpha_{e-h}(\lambda)$  the band-to-band absorption coefficient, and  $\alpha_n(\lambda)$  and  $\alpha_p(\lambda)$  are the defect absorption coefficients given by

$$\alpha_n(\lambda) = f_t N_t \sigma_n^{\text{opt}}(\lambda) \quad \text{and} \quad \alpha_p(\lambda) = (1 - f_t) N_t \sigma_p^{\text{opt}}(\lambda) \quad (8)$$

with  $f_t$  is the occupation probability of the impurity level. The free carrier absorption  $\alpha_{fc}(\lambda)$  is given by [16]

$$\alpha_{fc}(\lambda) = C_{fc}^n \lambda^2 n + C_{fc}^p \lambda^2 p \quad (9)$$

where  $C_{fc}^n$  and  $C_{fc}^p$  are empirical parameters.

In this study, we considered only band-to-band absorption  $\alpha_{e-h}(\lambda)$  and the defect absorption  $\alpha_n(\lambda)$  and  $\alpha_p(\lambda)$ ; free carrier

absorptions are not yet implemented in SCAPS. The importance of free carrier absorption was estimated a posteriori in Fig. 2, where the calculated IPV contributions  $\alpha_n$  and  $\alpha_p$  to the total absorption are compared to the literature data of the band-to-band and free carrier absorption. It is seen that  $\alpha_{fc}$  does not significantly contribute to  $\alpha_{\text{tot}}$  in the entire wavelength range under consideration. It should be noted that this absorption process is important in heavily doped semiconductors, and does not create electron-hole pairs so it gives no contribution to the photocurrent.

### 3. Results and discussion

The GaAs solar cell, which we have studied, is a  $p^+-n-n^+$  structure, in which Cu impurities are incorporated in the base region. We assume that the base region contains both a shallow background donor-type dopant as well as the acceptor-type IPV impurity copper. Also finite surface recombination velocities for

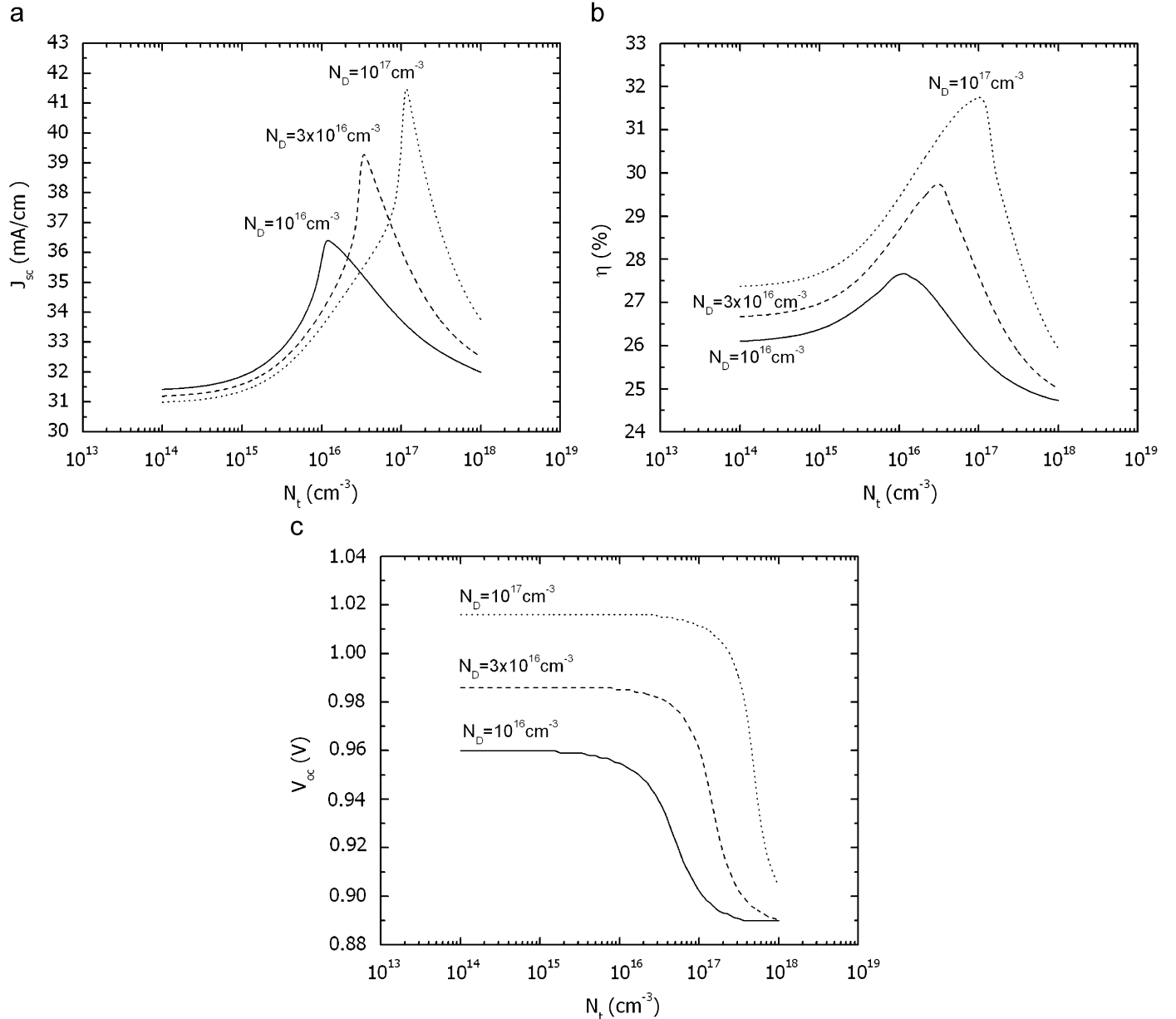


**Fig. 3.** Solar cell parameters of an IPV GaAs solar cell as a function of the Cu(B) impurity concentration  $N_t$  calculated for  $N_D = 10^{17} \text{ cm}^{-3}$ . The internal reflections are set to  $R_f = 0.999$  and  $R_b = 0.9999$  (a) short-circuit current density  $J_{sc}$ ; (b) conversion efficiency  $\eta$ ; and (c) open-circuit voltage  $V_{oc}$ .

electrons and holes are assumed. The doping concentration and the thicknesses of the different layers are, if not stated else, as follows:  $N_A = 10^{18} \text{ cm}^{-3}$ ,  $d = 0.5 \mu\text{m}$  for the  $p^+$  layer;  $N_D = 10^{17} \text{ cm}^{-3}$ ,  $d = 3.5 \mu\text{m}$  for the  $n$ -base layer and  $N_D = 10^{18} \text{ cm}^{-3}$ ,  $d = 2 \mu\text{m}$  for the  $n^+$  layer.

The parameters used in the simulation are given in Table 1. We used the model of Lucovsky to calculate the optical cross sections for electrons and holes, which needs the input of the four parameters: refractive index  $n$  of the semiconductor, the effective mass  $m_n^*$  and  $m_p^*$  of the carriers, and the effective field ratio  $E_{\text{eff}}/E_0$  which represents the ratio between the electric field at the impurity and the electric field of the incident wave [8].

The absorption coefficient  $\alpha_{e-h}(\lambda)$  for gallium arsenide is taken from Ref. [23]. The solar cell is assumed to be operating under global AM1.5 illumination and a temperature of 300 K. Light trapping is incorporated with a substantial effect, which corresponds to internal reflection at the back and the front close to unity.

### 3.1. Effect of impurity defect concentration

In this section, we assume that the band gap of the base layer contains only the Cu(B) defect level, and we calculate the solar cell parameters as function of the impurity concentration for different base doping concentrations  $N_D = 10^{16}$ ,  $3 \times 10^{16}$  and  $10^{17} \text{ cm}^{-3}$ . Fig. 3a–c, shows the short-circuit current density, efficiency and open-circuit voltage of the solar cell, respectively, as a function of the Cu(B) concentration  $N_t$ . The short-circuit current density and efficiency increase with increasing  $N_t$  only when  $N_t \leq N_D$ . In the previous work [6], we showed that the generation current due to the IPV effect is governed by the slowest optical process, which in this case is the electron transition from the impurity to conduction band described by  $\sigma_n^{\text{opt}}(\lambda)$ . At impurity densities above the shallow doping density in the base ( $N_t > N_D$ ), the impurity defect level is not fully occupied. The transition rate from the valence band to the defect level is then increased, which in turn reduces the photon flux available for the electron photoemission process from the defect to the conduction band.

The open-circuit voltage decreases but by keeping moderate values with increasing impurity concentration. This effect is due to the particular choice of the structure. It was recognized that the  $n^+$  layer near the base region, can safeguard a reasonable value of the built-in voltage and the open-circuit voltage [2].

In practice, there are limits to the application of high copper concentrations to obtain a substantial IPV effect. It was established that for low copper concentrations, the GaAs base semiconductor remains  $n$ -type and conducting, but turns to  $p$ -type at high Cu concentrations due to a compensation effect. Also, the density of the Cu impurities is effectively limited by the solid solubility of Cu in GaAs, which is about  $5 \times 10^{16} \text{ cm}^{-3}$  [20]. Finally, it is worth noting that at impurity concentrations exceeding  $10^{17} \text{ cm}^{-3}$  the SRH formalism as used here becomes inaccurate due to the onset of degeneration and other heavy doping effects.

### 3.2. Effect of light trapping

As discussed above, in our model all effects of the optical management of the cell are incorporated in the values of the internal reflection  $R_f$  at the front and  $R_b$  at the back of the cell. The effect of these reflection parameters on the short-circuit current is illustrated in Fig. 4. It is evident that the maximum IPV effect (a  $J_{sc}$  gain of  $\Delta J_{sc} \approx 9 \text{ mA/cm}^2$  with the parameters of Fig. 4) is only obtained for unphysical values  $R_f = R_b = 1$ . Nevertheless, a substantial IPV effect of e.g.  $\Delta J_{sc}$  exceeding  $2 \text{ mA/cm}^2$  can already be obtained at a high value of the reflection coefficients,  $R_f$  and

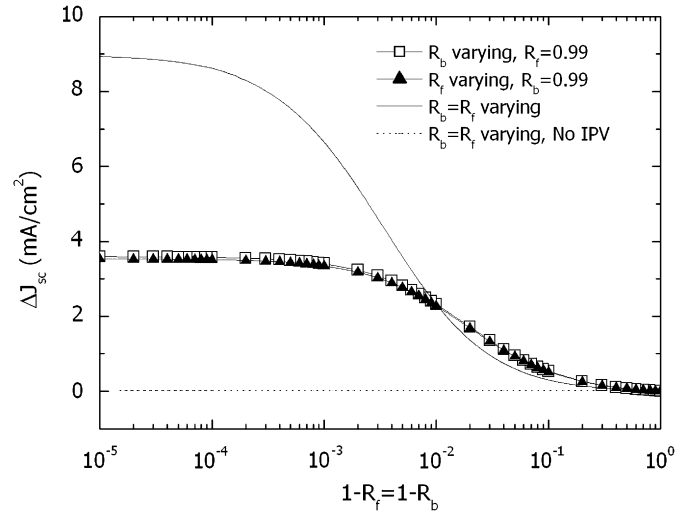


Fig. 4. Effect of the internal reflections  $R_f$  and  $R_b$  on the short-circuit current  $J_{sc}$ . The short-circuit current IPV gain  $\Delta J_{sc}$  is referred to the situation where no IPV effect is present. Calculated for  $N_D = N_t(B) = 10^{17} \text{ cm}^{-3}$ .

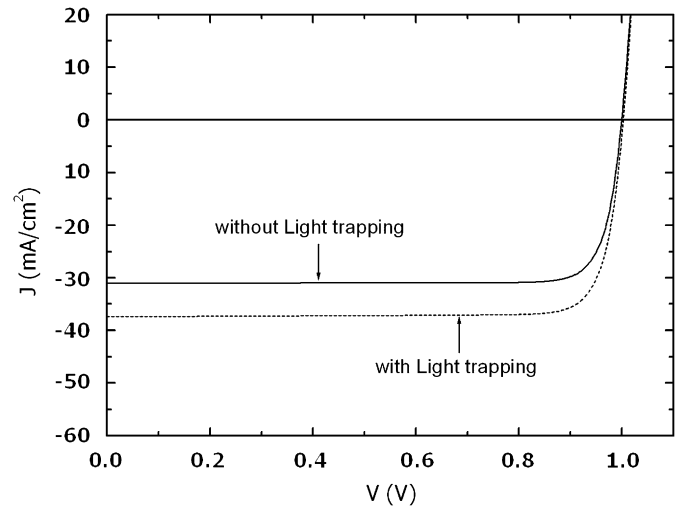


Fig. 5. Current–voltage curve  $J(V)$  of an IPV GaAs solar cell with Cu(B) impurity density  $N_t = 3 \times 10^{16} \text{ cm}^{-3}$ , calculated with ( $R_f = R_b = 0.9999$ ) and without ( $R_f = R_b = 0$ ) light trapping.

$R_b > 0.99$ . It is also verified in Fig. 4 that when no IPV effect is taken into account, the effect of a high value of  $R_f$  and  $R_b$  is very marginal:  $\Delta J_{sc} = 7 \mu\text{A/cm}^2$  only.

Fig. 5 compares the current–voltage curve of the IPV GaAs solar cell for  $N_t = 3 \times 10^{16} \text{ cm}^{-3}$ , with and without light trapping, respectively. With the parameters of Fig. 5, the IPV effect with light trapping results in a  $J_{sc}$  gain of about  $\Delta J_{sc} = 6 \text{ mA/cm}^2$  without any appreciable loss of  $V_{oc}$  or FF.

The potential benefits of light trapping in GaAs solar cells can be summarized in the following three features:

Increase optical absorption by maximizing the path length of weakly absorbed photons, which results in an increase of minority carrier's photogeneration.

Using a base layer of a thickness smaller than the minority carrier diffusion length, which improves the collection efficiency of the solar cell.

Increase photon recycling effects by optically confining photons generated by radiative recombination.

Many approaches are possible to implement light trapping in GaAs solar cells. One of the simplest implementations of this concept is planar back reflector, ensuring that weakly absorbed photons will cross the cell twice. This approach is compatible with most solar cells fabrication technologies, and can be realized by epitaxial lateral overgrowth or by incorporating a Bragg mirror reflector between the solar cell and the substrate. The first approach gives a reflection of about 50% at normal incidence, whereas the second gives a high reflection ( $>95\%$ ) [24]. Other researchers have proposed a Bragg reflector structure consisting e.g. of thin alternating layers of AlAs and  $(\text{Al}_x\text{Ga}_{1-x})\text{As}$ . This structure is reported to “reflect nearly 100% of long-wavelength photons” [25]. The implementation of such a Bragg reflector in a conventional heteroface cell would enhance the efficiency by approximately 1% absolute [25].

Another scheme to increase light trapping efficiency is by texturing the back mirror to scatter the reflected light. The usual approach is to model the textured back mirror as a Lambertian

reflector [26]. Texturing front and back surfaces can provide a high degree of light trapping, leading to high internal reflection coefficients. A discussion of possible experimental realisations, and of the practical limits that can be achieved, however, is beyond the scope of this paper.

### 3.3. GaAs solar cells with two impurity levels

The various energy levels introduced by copper impurities in the GaAs band gap are of different nature. Usually, the levels at 0.14 eV (‘Cu(A) level’) and 0.40 eV (‘Cu(B) level’) above the valence band edge are attributed to one  $\text{Cu}_{\text{Ga}}$  acceptor-type defect (i.e. substitutional copper at a gallium site), which can be singly or doubly occupied [9], though other interpretations are reported as well [13]. The other dominant Cu level at 0.24 eV above the valence band edge can be attributed to a variety of Cu-related defect complexes [9]; we call it here the Cu(C) level. It follows that the occupation and recombination of the Cu(A) and Cu(B) levels should not be described by the classical SRH formalism [10,27], but by the Sah and Shockley [28], theory for multiple charged

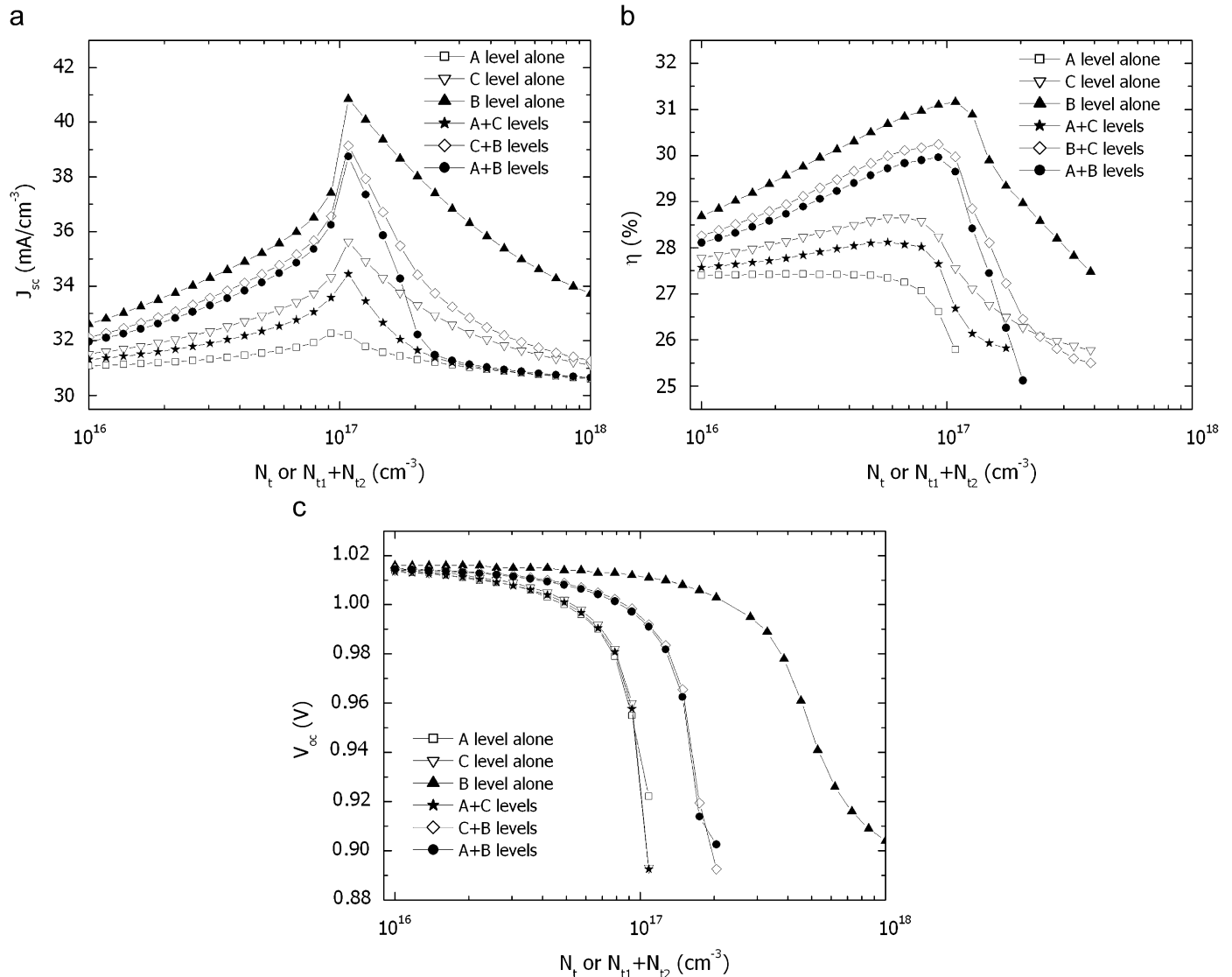


**Fig. 6.** Solar cell parameters of an IPV GaAs cell with one or two IPV levels present. Calculated for a base doping density  $N_D = 10^{17} \text{ cm}^{-3}$  and for internal reflection  $R_f = R_b = 0.999$ . With one level (e.g. A) present, the abscissa means  $N_t = N_t(A)$ ; with two levels present (e.g. A and B), the abscissa means  $N_t = N_t(A) + N_t(B)$ , with  $N_t(A) = N_t(B)$ . (a) Short-circuit current  $J_{sc}$ ; (b) conversion efficiency  $\eta$ ; and (c) open-circuit voltage  $V_{oc}$ .



defects; this theory has been presented conveniently for two levels/three charge states e.g. in Ref. [29].

We first pointed out that the occupation and recombination in such states can accurately be described by the more simple SRH formalism, provided that one attributes the same density  $N_t$  to both levels, and that one shifts the 0/–1 level (here the Cu(A) level) over an energy  $kT \ln(2) \cong 17$  meV towards the valence band, and the –1/–2 level (here the Cu(B) level) with  $kT \ln(2)$  towards midgap. In view of the large uncertainties about the energy levels in the literature, this small shift can be neglected.

To our knowledge, SCAPS is the only solar cell simulator available that treats the IPV effect. It has however also limitations: one can input three recombination mechanisms only. Since one is needed to adjust the recombination and the open-circuit voltage to a realistic value, only two IPV levels are available, and hence we cannot examine the influence of all three copper levels Cu(A), Cu(B) and Cu(C) simultaneously. Thus we will first examine the influence of two IPV levels, and compare the result with the effect of one IPV level. This is done in Fig. 6a–c. For only one level present, one can see that the IPV effect is more pronounced as the level is deeper, thus the largest IPV effect is with the Cu(B) level. This confirms results in Ref. [4]. When two levels are present, the IPV effect is somewhat lower than the IPV effect with only the deepest of the two levels present, e.g. the curves for the B+A or the B+C levels are somewhat below the curve for the ‘only B level’.

It is important to note that in the case of two impurity levels as treated here, only direct transition between a trap and the conduction and valence bands are considered. The reason is that the occurrence of transitions of electrons between levels requires the distance  $d$  between neighbouring traps to be small enough to allow for tunnelling ( $d < 5$ – $10$  nm) corresponding to high concentration doping. This is not the case in our calculation where we considered low concentrations due to the limited solubility of Cu in GaAs.

When we adopt the interpretation that the Cu(A) and Cu(B) levels originate from one single substitutional Cu impurity with two charge states, only A+B combination in Fig. 6 is physically possible. We thus further explore this case.

However, if we assume that concentration of copper impurity in each level is equal to that in only one level, e.g. in Fig. 6 comparing B level alone for  $N_t = 3 \times 10^{16} \text{ cm}^{-3}$  with A+B levels for  $N_t = 6 \times 10^{16} \text{ cm}^{-3}$  we find that the IPV effect gives an improvement in the short-circuit current density in the presence of A+B, but at the same time a decrease in the open-circuit voltage higher

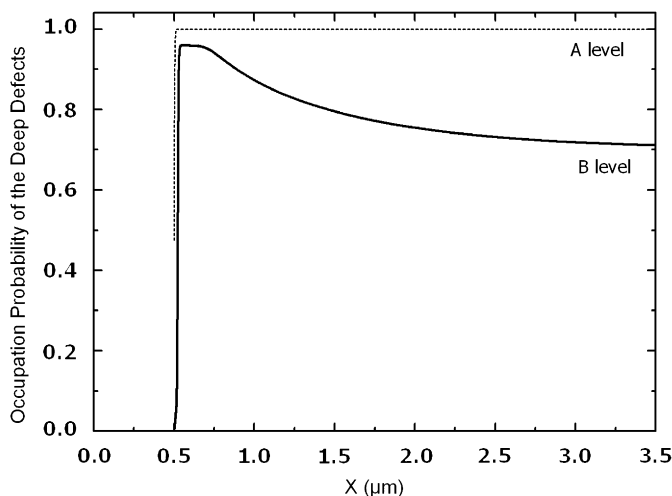


Fig. 7. Occupation probability of the Cu impurity levels A and B in an IPV GaAs solar cell calculated for  $N_t(A) = N_t(B) = 3 \times 10^{16} \text{ cm}^{-3}$  and  $R_f = R_b = 0.9999$ .

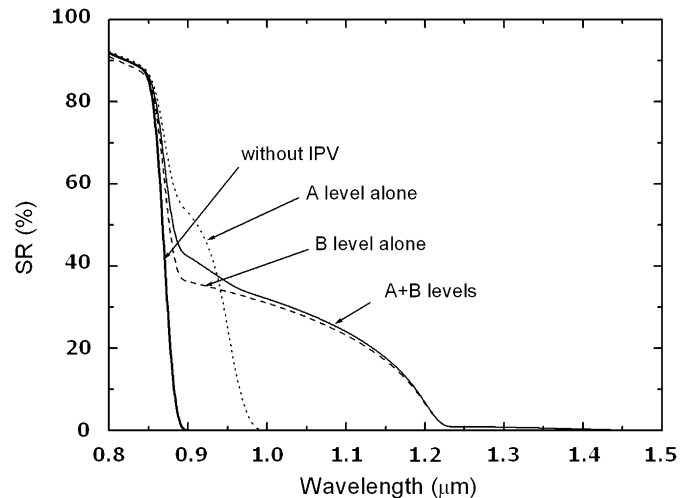


Fig. 8. Spectral response curve of the IPV GaAs solar cell with and without Cu impurity levels A and B calculated for  $N_D = 10^{17} \text{ cm}^{-3}$ ,  $N_t(A) = N_t(B) = 3 \times 10^{16} \text{ cm}^{-3}$  and  $R_f = R_b = 0.9999$ .

than in the presence of only the level B. This is due to the increase of recombination in the solar cell, which increases more drastically when the concentration of the defects is around the base layer doping.

In Fig. 7 we calculated occupation probability of the deep levels in the base region of the GaAs solar cell, for  $N_t = 3 \times 10^{16} \text{ cm}^{-3}$  and  $N_D = 10^{17} \text{ cm}^{-3}$ . From this figure we see that the lower energy level, which corresponds to Cu(A) is more completely occupied than the higher energy level Cu(B) since this latter is the deeper one (close to the energy Fermi level).

Fig. 8 shows the spectral response of the solar cell, in the four following cases: a solar cell without IPV, with Cu(A), with Cu(B) and with the two defect levels. It is confirmed that the contribution of the IPV effect to the short-circuit current  $J_{sc}$  comes from sub-bandgap absorption in the solar cell, which results in an extension of the infrared response, especially between  $\lambda = 873$  and  $1250$  nm. The presence of Cu(A) alone gives an improvement of the spectral response at  $873 \leq \lambda \leq 1000$  nm while Cu(B) improves the spectral response at wavelengths  $873 \leq \lambda \leq 1250$  nm. The curve with light trapping but with no IPV effect present almost exactly coincides with the curve for no light trapping (not shown in Fig. 8).

#### 4. Conclusion

We used a new version of simulator SCAPS to study the impurity photovoltaic (IPV) effect in a wide band gap solar cell (GaAs), containing three Cu acceptor impurity levels: Cu(A) at  $E_v + 0.14$  eV, Cu(B) at  $E_v + 0.40$  eV and Cu(C) at  $E_v + 0.24$  eV.

We showed that a good light management, ensuring internal reflection coefficients exceeding 99%, is needed to observe any IPV effect at all. The IPV effect becomes appreciable ( $\Delta J_{sc} > 8 \text{ mA/cm}^2$  and  $\Delta \eta > 5\%$ ) if higher values of the internal reflection coefficients were possible. The IPV effect extends the spectral sensitivity in the sub-bandgap range from 870 nm to about 1250 nm.

Our calculations show that the copper level should be kept fully occupied with electrons, in order to take maximal profit of the IPV effect. Therefore, the copper concentration should be close to, but not exceed the base doping.

Contribution of each level alone and also a combination of two different levels was examined. It is shown that when two levels are present, the IPV effect is higher with only the deepest level present. Physically, the two levels Cu(A) and Cu(B) are the most

likely to occur together. We showed that, when this combination is compared to only the Cu(B) level present, the IPV effect gives an improved short-circuit current but a decreased open-circuit voltage, due to increase recombination in the solar cell.

## Acknowledgements

This work is partly supported by Algerian ministry of higher education and research (CNEPRU Project no. D0801/01/05) and by the Research Fund of the University of Gent (BOF-GOA).

## References

- [1] M.J. Keevers, M.A. Green, Efficiency improvements of silicon solar cells by impurity photovoltaic effect, *J. Appl. Phys.* 75 (1994) 4022.
- [2] M. Schmeits, A.A. Mani, Impurity photovoltaic effect in c-Si solar cells. A numerical study, *J. Appl. Phys.* 85 (1999) 2207.
- [3] S.Zh. Karazhanov, Impurity photovoltaic effect in indium-doped silicon solar cells, *J. Appl. Phys.* 89 (2001) 4030.
- [4] G. Beaucarne, A.S. Brown, M.J. Keevers, R. Corkish, M.A. Green, The impurity photovoltaic (IPV) effect in wide-bandgap semiconductors: an opportunity for very-high-efficiency solar cells?, *Prog. Photovolt. Res. Appl.* 10 (2002) 345.
- [5] S. Khelifi, J. Verschraegen, M. Burgelman, A. Belghachi, Numerical simulation of impurity photovoltaic effect in silicon solar cells, *Renew. Energ.* 33 (2008) 293.
- [6] J. Verschraegen, S. Khelifi, M. Burgelman, A. Belghachi, Numerical modelling of the impurity photovoltaic effect (IPV) in SCAPS, in: *Proceedings of the 21th European Photovoltaic Solar Energy Conference*, Dresden, Germany, 2006, pp. 396–399.
- [7] M. Burgelman, P. Nollet, S. Degraeve, Modelling polycrystalline semiconductor solar cells, *Thin Solid Film* 361–362 (2000) 527.
- [8] G. Lucovsky, On the photoionization of deep impurity centers in semiconductors, *Solid State Commun.* 3 (1965) 299.
- [9] A.G. Milnes, *Deep Impurities in Semiconductors*, Wiley, New York, 1973.
- [10] S.M. Sze, *Semiconductor Devices, Physics and Technology*, Wiley, New York, 1985.
- [11] T.D. Dzhanfarov, M. Sirin, S. Akciz, Photoelectrical characteristics of GaAs p-n junctions formed by Cu photostimulated diffusion, *J. Phys. D* 31 (1998) L17.
- [12] C.H. Henry, D.V. Lang, Non radiative capture and recombination by multi-phonon emission in GaAs and GaP, *Phys. Rev. B* 15 (1997) 989.
- [13] K. Leosson, H.P. Gislason, Thermal and electrical of Cu-related acceptors in Li- and H-passivated GaAs, *Physica Scripta T* 69 (1997) 196.
- [14] P.N.K. Deenapanray, V.A. Coleman, C. Jagadish, Electrical characterization of impurity-free disordered p-type GaAs, *Electrochem. Solid-State Lett.* 6 (2003) G37.
- [15] P.N.K. Deenapanray, M. Petracic, C. Jagadish, M. Krispin, F.D. Aurret, Electrical characterization of p-GaAs epilayers disordered by doped spin-on-glass, *J. Appl. Phys.* 97 (2005) 1.
- [16] D.K. Schroder, R.N. Thomas, J.C. Swartz, Free carrier absorption in silicon, *IEEE Trans. Electron Devices* ED-25 (1978) 254.
- [17] S.M. Sze, *Modern Semiconductor Device Physics*, Wiley, New York, 1998.
- [18] J.J. Liou, W.W. Lang, Comparison and optimization of the performance of Si and GaAs solar cells, *Sol. Energy Mater. Sol. Cells* 28 (1992) 9.
- [19] S.P. Tobin, S.M. Vernon, C. Bajgar, S.J. Wojtczuk, M.R. Melloch, M.S. Lundstrom, K.A. Emery, Assessment of MOCVD- and MBE- grown GaAs for high-efficiency solar cell applications, *IEEE Trans. Electron Devices* 37 (2) (1990) 469.
- [20] B.H. Yang, D. Seghier, H.P. Gislason, Compensation mechanism and transport behaviour of semi-insulating GaAs:Cu, in: *Proceedings of Semiconducting and Semi-insulating Materials Conference*, 29 April–3 May 1996, Toulouse, France, IEEE, 1996, pp. 163–166.
- [21] P. Blood, J.J. Harris, Deep states in GaAs grown by molecular beam epitaxy, *J. Appl. Phys.* 56 (4) (1984) 993.
- [22] S. Brehme, R. Pickenhain, An acceptorlike electron trap in GaAs related to Ni, *Solid State Commun.* 59 (1986) 469.
- [23] S. Adachi, *Optical Constants of Crystalline and Amorphous Semiconductors*, Numerical Data and Graphical Information, Kluwer Academic Publishers, USA, 1999.
- [24] C.B. Honsberg, A.M. Barnett, Light trapping in thin film GaAs solar cells, in: *Proceedings of 22nd IEEE Photovoltaic Specialists Conference*, October 1991, Las Vegas, NV, IEEE, New York, 1991, pp. 262–267.
- [25] L.D. Partain, *Solar Cells and their Applications*, Wiley, New York, 1995.
- [26] A. Goetzberger, Optical confinement in thin silicon solar cells by diffuse back reflectors, in: *Proceedings of 15th IEEE Photovoltaic Specialists Conference*, IEEE 1981, pp. 867–870.
- [27] W. Shockley, W. Read, Statistics of the recombination of holes and electrons, *Phys. Rev.* 87 (1952) 835.
- [28] C.T. Sah, W. Shockley, Electron-hole recombination statistics in semiconductors through flaws with many charge conditions, *Phys. Rev.* 109 (1958) 1103.
- [29] R. Schropp, M. Zeman, *Amorphous and Microcrystalline Silicon Solar Cells: Modelling, Materials and Device Technology*, Kluwer Academic Publishers, Boston, 1998 (pp. 133 and 138–140).